IUGG General Assembly
Boulder, USA, july 2, 1995

International Association of Geodesy

Symposium "GEODESY IN SOUTHEAST ASIA"

TIDAL GRAVITY MEASUREMENTS IN SOUTHEAST ASIA

P. Melchior, O. Francis and B. Ducarme
Observatoire Royal de Belgique
Avenue Circulaire 3
B-1180 Bruxelles, Belgium

Abstract

Since 1974, 17 temporary tidal gravity stations have been established in Southeast Asia. Most of them were installed by the Royal Observatory of Belgium in the framework of the Trans World Tidal Gravity Profile. The observations are compared to an Earth's model with liquid core and oceans using the Schwiderski and the Grenoble cotidal maps.

The calibration problems are carefully treated. The results show that the tidal gravity effects for the principal semi-diurnal M_2 tide are modeled with a precision of 2.5 microgal which is not satisfactory. On the contrary the lunar diurnal O_1 tide is modeled almost perfectly with only few exceptions which eliminates the hypothesis of instrumental phase errors. Two reasons can be invoked. Either a deficiency in the M_2 turbulent cotidal map of Java sea and neighbouring seas where not less than 8 or 10 amphidromic points make these maps very complicate, either a regional anomaly in the earth tides deformations as reflected by the presence of the largest geoid bump.

1. Introduction

The new techniques now available in Geodesy and Geodynamics reach such a high precision in positioning and gravity (absolute as well as differential) measurements that it becomes compulsory to introduce corrections for the tidal effects with a precision better than one percent.

Tidal effects are particularly important (Table 1) and difficult to calculate or modelize in Southeast Asia.

During the period 1973-1981 the Royal Observatory of Belgium, assisted by the International Centre for Earth Tides in Brussels, has established not less than 15 temporary tidal gravity stations in this area (Table 2). Two stations were also established in 1957 at Saigon and Baguio by the University of California (Los Angeles) but we have not been able to check or revise the calibration of the two LaCoste Romberg n° 2 and n° 5 instruments used (Melchior 1994).

Another LaCoste Romberg (n° 305) was installed in 1977-78 at Baguio by the International Latitude Observatory in Mizusawa, Japan but we were also unable to check the calibration. Nevertheless the results given in Table 6 for this instrument look reliable.

Among the other stations established by the Brussels team, Manila and Port Moresby stations are not too reliable because of some difficulties encountered in the calibration of the LaCoste Romberg gravimeter n° 3.
From a complete revision of all existing data, Melchior (1994), using 215 stations almost free of obvious anomalies or calibration errors, concluded for the classical amplitude factor δ (δ = 1 + h - 3/2k; h, k: elastic Love numbers) and phase α:

$$\delta\ (M_2) = \quad 1.1564 \pm 0.0005$$

$$\alpha\ (M_2) = -\ 0.09° \pm 0.03°\ \text{(minus is a lag)},$$

while the calibrations in amplitude of the different instruments, made at the Brussels fundamental station, are estimated to be better than 1%.
This means that, at the equator, a maximum error of 0.8 μgal is possible on the M_2 measured amplitude and less than 0.2 μgal on the O_1 measured amplitude.

2. Semi-diurnal tides in Southeast Asia

It is well known that while the tesseral diurnal tidal gravity waves vanish, the sectorial semi-diurnal components are maximum at the equator. According to Table 1 they can reach a peak to peak amplitude of 340 microgals at some epochs when the four main waves are adding their effects.
One has also to add the amplitudes of the attraction and loading due to the oceanic tides acting at the same frequencies which, in principle, can be evaluated on the basis of the Schwiderski corange-cotidal map which had been recommended as a working standard by the IAG Commission on Earth Tides. These effects are given in the Table 4 for all the Southeast Asia stations where tidal gravimeters have been installed. They are not negligible at all, reaching more than 20 microgals peak to peak at some places (notably Kupang, Timor).

However the oceanic tides behaviour is extremely complicate in the Indonesian area, the Schwiderski and Grenoble maps of the main wave M_2 exhibiting respectively not less than eight and ten amphidromic points situated along a line meandering successively between the Malay peninsula and Cambodge, between Java and Borneo (Kalimantan), and between Australia and Timor, Papua (see figure 1 and Table 5).

The usual interpretation procedure consists, for each tidal wave, to consider the result of the harmonic analysis of the observations as a vector **A** (A, α) defined by the amplitude A (in microgal) and its phase difference α with respect to the local phase deduced from the tidal gravity potential.

For the different tidal vectors related to one tidal wave under consideration (in this paper the semi-diurnal sectorial wave M_2), we will use here the same notations as in previous papers (Melchior, 1983) and illustrated by Fig. 2.

R (R, 0) is the earth model computed response to the luni-solar tidal potential; it contains as a factor the combination of Love numbers δ = 1 + h - (3/2)k corresponding to the Earth model considered.

A (A, α) is the observed tidal response as obtained by least squares analysis of the observations.

B (B, β) = **A** - **R** is the first residue vector which contains mainly the oceanic tides contribution to the gravity variations.

L (L, λ) is the oceanic contribution calculated by the Farrell (1972) procedure using the Schwiderski cotidal-corange maps (1980) (Francis and Dehant, 1987).

X (X, χ) = **B** - **L** = **A** - **R** - **L** is the final residue vector expected to represent the observations noise (about 0.3 μgal for the M_2 wave). In number of cases, however, it greatly exceeds this noise level.

From the Data Bank of ICET which contains the results of some 350 tidal gravity stations all around the world, Melchior (1995 fig. 3) obtained the following means and standard deviations:

$$X \cos \chi\ (M_2) = + 0.002 \pm 0.045\ \mu\text{gal}$$

$$X \sin \chi\ (M_2) = - 0.154 \pm 0.028\ \mu\text{gal}$$

Obviously the results in Southeast Asia given in Table 6, from Colombo (Sri Lanka) in the West to Port Moresby (Papua) in the East, are by very far greater than these mean values and than the observation noise (0.3 μgal - Melchior, 1994) as well.

This could be interpreted as due to the complicate behaviour of the M_2 oceanic tide around the islands of the Indonesian Archipelago.

But a check with a more recent and more precise corange-cotidal map is needed to endorse such a statement. Such a map, recently produced by the Grenoble team from a purely hydrodynamic model (Le Provost et al., 1995) has been made available to us. This map is constructed on a 0.5° x 0.5° grid, thus four times more detailed than the Schwiderski map which is based upon a 1° x 1° grid.
One could expect therefore some improvement in the description of the tides around the many islands of Indonesia, notably inside the Java sea, Banda sea and the Timor and Savu seas. We used it to calculate new **L** vectors and, as a result, new **X** vectors which are given in the same Table 6 as the Schwiderski **L**, **X** vectors for the 17 stations. The situation is, at first sight, not different as at 5 stations only has the X amplitude significantly decreased (by at least 0.5 μgal) with respect to the Schwiderski results (Kota Kinabalu, Manila, Bandung, Manado, Jaya Pura).

Taking simple arithmetic means we observe a mean B amplitude of 2.8 μgal and a mean X amplitude of 1.7 μgal after correction either with the Schwiderski map or with the Grenoble map.
One should also point out that the observed amplitudes of the M_2 oceanic tide is less than 30 cm in all harbours close to our stations at the exception of Kuala Lumpur, Kupang and Darwin (Table 7), three places where the X residue is not more than 1 μgal.
In Table 7 we compare the phases measured in harbours which are close to our tidal gravity stations with the phases listed in the Schwiderski tables. The agreement is generally very good as Schwiderski, most probably, used the same data as us (Schwiderski 1979).
The high number of amphidromic points in both maps (Table 5) is evidence of the low amplitudes of the oceanic tides in this area.

When we consider the difference in the loading amplitudes and phases obtained from both maps as given in the last columns of Table 6 we observe that the difference in amplitude is comprised between 0.5 and 1.2 microgal. However there are two groups of stations for what concerns the phases:

- a group of 8 stations situated to North, North East ($\lambda \leq 107°$ E) of the equator with a mean difference 0.6 μgal and a phase around - 150°

- a group of 9 stations situated to the South West ($\lambda \rangle 114°$ E) with a mean difference 0.8 μgal and a phase around + 75°,

the two groups being separated by the meandering line connecting the amphidromic points of the Schwiderski and Grenoble maps mentioned before. The corresponding load and attraction difference between these two groups is 1.3 μgal with a -122.5° phase difference (Schwiderski map - Grenoble map). This difference is obviously related to a shift of the amphidromic points of one map with respect to the other.

Anyway the residual amplitudes X remain quite high as most of them are higher than one microgal which is difficult to explain by errors in the computation of the oceanic tides effects in an area where there are so many amphidromic points (null tidal amplitude).
A special investigation was performed by one of our students (Mouzon, 1981) about the effect of the Malacca Strait tides upon the stations Penang and Kuala Lumpur. She used the British Admiralty Map established for this important navigation Channel.
Her results, applied to the Schwiderski residues X given in Table 6 are :

2550	Kuala Lumpur	X (Schwiderski)	1.10	99°
		Admiralty map	0.61	41°
		difference	0.94	133°
2551	Penang	X (Schwiderski)	1.51	164°
		Admiralty map	1.40	- 173°
		difference	0.58	97°

There is a real improvement for Penang island which is at the Northern exit, 280 km broad, of the Malacca Strait with a local oceanic tidal amplitude of 57 cm (Table 7).
For Kuala Lumpur which is South of Penang, in the narrow part (60 km) of the Strait, there is practically no improvement. One should point out the very large amplitude, 136 cm, of the M_2 oceanic tide at the closest harbour Port Klang (Table 7) which is most probably responsible for a strong local effect. On the opposite side of the Strait, along the Sumatra coast, the amplitude of the M_2 wave increases from 46 cm at the Northern entry to 168 cm in front of Kuala Lumpur and then decreases to 75 cm in front of Johore, Southern exit.

Considering that the "in phase" components (X cos χ) are all strongly positive for both solutions (Schwiderski and Le Provost) and quite larger than the "out of phase" components (X sin χ) in all Indonesian stations (at the exception of Jaya Pura - North New Guinea) it could be temptating to raise the problem of effects due to lateral heterogeneities (Melchior 1995) in this Indonesia area which is the contact of two tectonic plates and the place with the world's biggest geoid bump (COSPAR 1994).

Only three stations amongst those installed in Southeast Asia are not coastal stations (D $\rangle$ 50 km): Chiang Mai, Bandung and Darwin but we have found informations about the heat flow only at Bandung and Darwin.
These two stations (neither the other 15 here reported) were not used by

Melchior (1995) in his attempt to confirms a correlation between heat flow and tidal residue X cos χ owing to the complicated behaviour of the oceanic tides.

We can see here that, even if the Grenoble map decreases the amplitudes of the residues at both places, they still remain positive at the level of one microgal which fits with the correlation suggested.

				X cos χ	
		D (km)	H	Schw.	Gren.
4100	Bandung	70	82	2.21	1.11
4210	Darwin	60	96	1.00	0.76

H : heat flow in milliwat m^{-2} (mean value 57)
X cos χ : microgal.

3. <u>The lunar diurnal wave O_1 in Southeast Asia</u>

As said before the diurnal waves vanish at the equator. It is therefore not appropriate to consider their amplitude factor δ and phase because the observed amplitudes are considerably affected by the attraction and loading of oceanic tides.

We therefore analyse here these oceanic effects by comparing in the Table 8 the B residue vector to the L oceanic vector and their difference X = B - L.

As shown in this table the oceanic effect has a minimum percentage to the total observed amplitude of 3% at Chiang Mai (highest latitude site: 18.79°) and maxima of 177% at Jaya Pura (latitude - 2.5°) and of 115% at Manado (latitude 1.45°).

Considering the small amplitudes of the B and L vectors - less than 3 μgal - the concordance between the phases β and λ is in general impressive, the only exceptions being Manila, Manado and Darwin.

This shows that:

1) the instrumental phase lags are well corrected

2) the O_1 Schwiderski corange-cotidal map better fits the observations than the M_2 map which may be attributed to the fact that there is less turbulence at the O_1 frequency (13.943°/hour) than at the M_2 frequency (28.984°/hour); there are indeed only three O_1 amphidromic points in this area instead of eight in the case of M_2 wave.

3) that tidal gravity measurements in the equatorial regions contain valuable and useful informations in the diurnal band also.

4. Acknowledgements

The authors wish to thank Prof. Jacub Rais, Director of the Indonesian National Agency for Survey and Mapping, Bakosurtanal for his deep interest and efficient help in the establishment of six successful tidal gravity stations in Indonesia.
Thanks are also expressed to our colleagues who helped us in the installations of the tidal gravity stations listed in Table 2.

References

Chueca, R., Ducarme, B., and Melchior, P., 1984.
Preliminary investigation about a quality factor of tidal gravity stations.
Bull. Inf. Marées Terrestres, 94: 6334-6337.

COSPAR, 1994.
Géoïde observé par les missions spatiales. Programme Spatial français, XXXe Assemblée Hambourg, page 29.

Francis, O. & Dehant, V., 1987.
Recomputation of the Green's functions for tidal loading estimation.
Bull. Inf. Marées Terrestres, 100 : 6962-6986.

Le Provost, C., Genco, M.L., Lyard, F., Vincent, P. and Canceill, P., 1995.
Spectroscopy of the World Ocean Tides from a Finite-Element Hydrodynamic model. J. Geophys. Res., Special TOPEX/POSEIDON ISSVE, in press.

Melchior, P., 1983.
The Tides of the Planet Earth.
Pergamon Press 2nd Edition 641 pages.

Melchior, P., 1994.
A new data bank for tidal gravity measurements (DB 92).
Physics of the Earth and Planetary Interiors, Vol 82 : 125-155.

Melchior, P., 1995.
An ongoing discussion about the correlation of tidal gravity anomalies and heat flow densities.
Physics of the Earth and Planetary Interiors, Accepted for publication, july 1994.

Melchior, P. and Ducarme, B., 1977.
Activities of the FAGS International Centre for Earth Tides (ICET) in the region between Thailand and Oceania.
Proc. Regional Geod. Networks for the Year 2000 Bandung, Indonesia : 172-190.

Melchior, P. and Ducarme, B., 1980.
Tidal Gravity Profiles 1973-1980
Bull. Observ. Marées Terrestres, Obs. Roy. Belgique, vol. IV, fasc. 5: 47-62.

Mouzon, J., 1981.
Etude des effets de surcharge océanique sur la croûte terrestre dans le détroit de Malacca.
Mémoire, Faculté des Sciences, Université Catholique de Louvain-la-Neuve, 180 pages.

Schwiderski, E., 1980.
On charting global ocean tides.
Rev. Geophys. Space Phys., 18: 243-268.

Schwiderski, E.W., 1979.
Global Ocean Tides, Part II: The Semi-diurnal principal Lunar Tide (M_2). Atlas of Tidal Charts and Maps.
Naval Surface Weapons Center TR 79-414, Dahlgren, Virginia 22448.

Schwiderski, E.W., 1981.
Global Ocean Tides, Part V: The diurnal principal Lunar Tide (O_1). Atlas of Tidal Charts and Maps.
Naval Surface Weapons Center TR 81-144, Dahlgren, Virginia 22448.

Table 1

Amplitudes of the Four Main Sectorial Semi-diurnal Waves (in μgal)

at the Equator

Wave		Period	Rigid Earth model	Elastic Earth model
M2	Main Lunar	12h 4206	75.07	87.08
S2	Main Solar	12h 0000	46.56	54.01
N2	Elliptic Lunar	12h 6583	14.37	16.67
K2	Luni-Solar declinational	11h 9672	9.51	11.03

Table 2 **Tidal Gravity Stations installed in Southeast Asia**

Station		Country	Instrument	Installation	Epoch	N	Q
2460	Colombo	Sri Lanka	G 765	Ducarme	1977-78	3744	8.0
2502	Chiang Mai	Thailand	G 084 L 008	Ducarme Poitevin Phiphitkun	1974 1982	4800	5.4
2501	Bangkok	Thailand	G 084	Melchior Ducarme	1973-74	2208	5.3
2551	Penang	Malaysia	G 765	Ducarme	1976	3600	5.8
2550	Kuala Lumpur	Malaysia	G 765	Melchior	1976-77	3744	12.0
2701	Saigon	Vietnam	L 005	Forbes	1957	912	6.0
4100	Bandung	Indonesia/Java	L 336	Ducarme	1976	4704	4.4
4210	Darwin	Australia	L 336	Melchior	1975-76	2688	1.6
4010	Baguio	Philippines	L 305	Nakai Sasaki	1978	2112	3.8
4011	Manila	Philippines	L 003	Melchior Ducarme	1973-74	2064	1.4
2555	Kota Kinabalu	East Malaysia Borneo	G 765	Ducarme	1977	3552	4.6
4105	Banjar Baru	Indonesia Borneo	L 008	Poitevin Matindas Mubroto	1979-80	4320	7.8
4111	Manado	Indonesia Sulawesi	L 336	Matindas	1978	2688	1.4
4120	Jaya Pura	Indonesia New Guinea	L 336	Ducarme Mubroto	1977-78	1968	0.9
4110	Ujung Pandang	Indonesia Sulawesi	L 336	Melchior	1976-77	3072	3.6
4115	Kupang	Indonesia Timor	L 008	Matindas Mubroto	1980-81	5616	6.5
4160	Port Moresby	Papua New Guinea	L 003	Melchior Ducarme	1974-75	3504	3.6

G : Geodynamics Gravimeter
L : LaCoste-Romberg Gravimeter
N : Number of hourly readings
Q : Quality factor (Chueca et al.1984)

Table 3 Wave M2 - Amplitude and Tidal Factors

Stations		Observed			Corrected for oceanic effects	
		Ampl	δ	α	δ*	α*
2460	Colombo	81.94	1.1085	0.86	1.1261	0.49
2502	Chiang Mai	77.05	1.1459	-0.58	1.1529	0.41
2501	Bangkok	80.98	1.1446	-0.32	1.1534	0.68
2551	Penang	83.86	1.1772	0.34	1.1738	0.27
2550	Kuala Lumpur	86.84	1.1613	0.43	1.1577	0.71
2701	Saigon	83.46	1.1531	-0.92	1.1617	-0.77
4100	Bandung	89.69	1.2132	-1.86	1.1902	-0.67
4210	Darwin	83.93	1.1772	0.34	1.1738	0.27
4010	Baguio	83.00	1.2020	-0.17	1.1664	0.31
4011	Manila	82.72	1.1780	-0.34	1.1437	0.05
2555	Kota Kinabalu	85.29	1.1496	-0.68	1.1420	-0.33
4105	Banjar Baru	88.49	1.1839	-0.14	1.1698	0.37
4111	Manado	92.30	1.2315	-0.40	1.1903	-0.43
4120	Jaya Pura	89.75	1.1989	-1.62	1.1736	-1.18
4110	Ujung Pandang	88.05	1.1856	-1.92	1.1986	-1.12
4115	Kupang	81.91	1.1275	-3.15	1.1751	-0.18
4160	Port Moresby	89.58	1.2271	-0.34	1.2280	0.59

Table 4 Oceanic Loading and Attraction effects according to Schwiderski Maps

		Principal Waves					
	Station	M2		N2		S2	
		μgal	degrees	μgal	degrees	μgal	degrees
2460	Colombo	1.44	158	0.18	-165	1.01	115
2502	Chiang Mai	1.44	-110	0.30	-106	0.59	-165
2501	Bangkok	1.57	-113	0.33	-110	0.71	-169
2551	Penang	1.51	-128	0.38	-121	1.01	177
2550	Kuala Lumpur	0.51	-58	0.13	-76	0.37	176
2701	Saigon	0.67	-160	0.18	-117	0.40	163
4100	Bandung	2.51	-49	0.49	-26	0.83	-116
4210	Darwin	0.24	22	0.11	49	0.16	-10
4010	Baguio	2.56	-16	0.44	-3	0.94	-32
4011	Manila	2.47	-13	0.43	1	0.93	-30
2555	Kota Kinabalu	0.78	-48	0.12	-33	0.18	-60
4105	Banjar Baru	1.32	-38	0.20	-26	0.26	-84
4111	Manado	3.08	0	0.54	14	1.78	-24
4120	Jaya Pura	2.02	-22	0.44	5	0.41	-13
4110	Ujung Pandang	1.59	-129	0.28	-121	0.62	170
4115	Kupang	5.67	-130	0.86	-121	3.08	170
4160	Port Moresby	1.49	-93	0.50	-61	1.13	-51

Table 5 **Amphidromic Points**

Tidal Wave M2

	Schwiderski Map			Area	Grenoble Map		
	latitude	longitude	rotation		latitude	longitude	rotation
				Gulf of Thailand	12.5°	100.5°	?
	8°	104.0°	CCW	Gulf of Thailand			
*	5°	106.5°	CCW	East of Malaysia	5.5°	105.5°	CCW
				Southeast of Malaysia	1.0°	106.5°	CCW
					-1.0°	108.0°	CCW
	-5°	111.5°	CW	Java Sea South of Borneo			
*	-6°	115.0°	CCW	Java Sea South of Borneo	-5.5°	114.0°	CCW
*	-13°	128.0°	CW	Timor Sea	-13.5°	127.0°	CW
				Arafura Sea	-6.5°	136.5°	CCW
	-10°	139.0°	CCW	Arafura Sea	-10.5°	139.0°	CW
*	-15°	140.0°	CCW	Gulf of Carpentaria	-14.5°	137.5°	CCW
				Coral Sea	-10.5°	143.5°	CW
	-10°	153.0°	CCW	Solomon Sea			

Tidal Wave O1

*	8°	103.0°	CW	Gulf of Thailand	8.0°	102.0°	CW
	-6°	110.5°	CW	Northern Coast of Java			
*	-13°	139.0°	CW	Gulf of Carpentaria	-13.0°	138.5°	?

CW : Clockwise
CCW: Counterclockwise
* : identical position on both maps

Table 6

					Observed		Schwiderski		Grenoble		Schwiderski map				Grenoble map				$X_c - X_s$	
NUM	STATION	LONG	LAT	D	B	β	L	λ	L	λ	X cosχ	X sinχ	X	χ	X cosχ	X sinχ	X	χ	amplitude	phase
2460	COLOMBO	79.87	6.90	3	4.01	162	1.44	158	1.46	148	-2.48	0.70	2.58	164	-2.58	0.47	2.62	170	0.25	-113
2502	CHIANG MAI	98.98	18.79	300	1.24	-141	1.44	-110	1.08	-93	-0.48	0.57	0.75	130	-0.90	0.30	0.95	162	0.50	-147
2501	BANGKOK	100.60	13.79	25	1.19	-158	1.57	-113	1.53	-89	-0.48	0.99	1.10	116	-1.12	1.08	1.56	136	0.64	-188
2551	PENANG	100.30	5.36	1	2.51	-162	1.51	-128	1.11	-139	-1.46	0.41	1.51	164	-1.55	-0.05	1.55	-178	0.47	-102
2550	KUALA LUMPUR	101.65	3.12	30	0.66	82	0.51	-58	1.18	19	-0.18	1.09	1.10	99	-1.03	0.27	1.06	165	1.18	-136
2701	SAIGON	106.70	10.78	60	1.44	-111	0.67	-160	0.05	160	0.11	-1.12	1.12	-84	-0.47	-1.36	1.44	-109	0.63	-157
4100	BANDUNG	107.63	-6.90	70	4.84	-37	2.51	-49	3.06	-26	2.21	-1.03	2.44	-25	1.11	-1.57	1.92	-55	1.22	-154
4210	DARWIN	131.13	-12.85	60	1.32	22	0.24	22	0.51	23	1.00	0.41	1.08	22	0.76	0.30	0.82	21	0.26	-155
																	MEAN		0.60	-147
4010	BAGUIO	120.58	16.41	25	3.33	-31	2.56	-16	2.10	-33	0.40	-1.01	1.09	-69	1.10	-0.57	1.24	-27	0.83	32
4011	MANILA OBS	121.07	14.64	20	1.35	-21	2.47	-13	1.84	-39	-1.15	0.09	1.15	176	-0.18	0.66	0.69	105	1.13	31
2555	KOTA KINABALU	116.07	5.95	2	1.28	-128	0.78	-48	0.85	-95	-1.31	-0.43	1.38	-162	-0.71	-0.16	0.73	-167	0.66	24
4105	BANJAR BARU	114.78	-3.33	20	1.79	-7	1.32	-38	1.58	-48	0.73	0.58	0.94	38	0.72	0.96	1.20	53	0.38	92
4111	MANADO	124.83	1.45	4	5.39	-7	3.08	0	4.12	-9	2.27	-0.66	2.36	-16	1.28	-0.04	1.28	-2	1.17	148
4120	JAYAPURA	140.67	-2.50	5	3.83	-41	2.02	-22	2.87	-40	1.01	-1.77	2.04	-60	0.67	-0.69	0.96	-45	1.14	107
4110	UJUNG PANDANG	119.63	-5.67	12	3.48	-58	1.59	-129	2.38	-122	2.85	-1.72	3.33	-31	3.10	-0.93	3.24	-17	0.83	72
4115	KUPANG	123.57	-10.20	1	5.14	-119	5.67	-130	6.76	-127	1.18	-0.17	1.19	-8	1.56	0.91	1.81	30	1.15	71
4160	PORT MORESBY	147.15	-9.41	5	4.92	-6	1.49	-93	3.13	-94	4.97	0.97	5.06	11	5.10	2.61	5.73	27	1.64	85
																	MEAN		0.79	76

D : Distance, in Km, to the sea shore
B, L, X are given in μgal
β, λ, χ are given in degrees

Table 7 Oceanic Tide M2 at closest Harbour

	Station	Long.	Lat.	Harbour	Long.	Lat.	A(cm)	α	α-2λ	Schwiderski
2460	Colombo	79.87	6.90	Colombo			17.6	50°	250°	252°
2502	Chiang Mai	98.98	18.79							
2501	Bangkok	100.60	13.79							
2551	Penang	100.30	5.36	Penang			56.8	354°	153°	
2550	Kuala Lumpur	101.65	3.12	Klang	101.23	3.00	136.2	132°	289°	
2701	Saigon	106.70	10.78	Anam Hatien	104.45	10.37	10.0	96°	247°	
4100	Bandung	107.63	-6.90	Jakarta	106.90	-6.10	5.3	350°	137°	
4210	Darwin	131.13	-12.85	Darwin			199.9	144°	242°	220°
4010	Baguio	120.58	16.41	San Fernando	120.30	16.60	7.6	273°	32°	32°
4011	Manila Obs.	121.07	14.64	Manila			20.0	305°	63°	55°
2555	Kota Kinabalu	116.07	5.95	Gaya	116.10	6.10	21.3	312°	80°	100°
4105	Banjar Baru	114.78	-3.33	Sungai Musang	114.50	-3.50	28.8	142°	273°	310°
4111	Manado	124.83	1.45	Gorontalo	123.10	0.50	14.5	115°	229°	280°
4120	Jayapura	140.67	-2.50	Hollandia			25.0	213°	292°	288°
4110	Ujung Pandang	119.63	-5.67	Macassar			8.0	70°	191°	200°
4115	Kupang	123.57	-10.20				45.8	317°	70°	48°
4160	Port Moresby	147.15	-9.41	Finsch Harb	147.80	-6.60	6.8	75°	139°	

Table 8 **Lunar Diurnal Tidal Wave O1 Observed Amplitudes and Residues**

	Station	Lat.	A	B	β	L	λ	X	χ	B/A %
4111	Manado	1.45	1.85	2.12	-124.6	1.77	-59.0	2.13	-173.7	115
4120	Jaya Pura	-2.50	1.23	2.18	-16.9	1.50	-19.1	0.68	-12.1	177
2550	Kuala Lumpur	3.12	4.06	0.97	-88.2	1.08	-89.3	0.11	80.4	24
4105	Banjar Baru	-3.33	4.84	2.23	-93.1	1.98	-83.8	0.43	-141.7	46
2551	Penang	5.36	6.60	1.18	-99.2	1.05	-83.3	0.34	-157.5	18
4110	Ujung Pandang	-5.67	7.71	2.73	-93.0	2.20	-89.5	0.54	-107.2	35
2555	Kota Kinabalu	5.95	8.19	3.26	-88.2	2.40	-78.3	0.99	-113.1	40
4100	Bandung	-6.90	8.57	1.46	-84.7	1.51	-73.9	0.28	-180.5	17
2460	Colombo	6.90	8.66	0.35	77.0	0.28	78.6	0.07	70.7	4
4160	Port Moresby	-9.41	10.65	0.96	4.9	1.60	-1.8	0.66	168.5	9
4115	Kupang	-10.20	14.17	2.79	-120.9	2.35	-94.9	1.23	-177.1	20
2701	Saigon	10.78	13.64	1.72	-79.5	1.96	-79.8	0.23	97.8	13
4210	Darwin	-12.85	16.90	1.46	152.3	1.12	-109.5	1.97	117.9	9
2501	Bangkok	13.79	17.02	0.60	-54.0	0.57	-50.7	0.05	-97.6	4
4011	Manila	14.64	17.41	1.92	-98.4	1.78	-54.8	1.38	-161.0	11
4010	Baguio	16.41	20.42	2.20	-57.4	1.94	-57.0	0.26	-60.3	11
2502	Chiang Mai	18.79	22.23	0.60	-62.4	0.43	-61.2	0.17	-65.5	3

A, B, L, X are given in μgals

β, λ, χ, are given in degrees

Table 9 **Oceanic Tide O1 at closest Harbour**

	Station	Long.	Lat.	Harbour	Long.	Lat.	A(cm)	α	α-λ	Schwiderski
2460	Colombo	79.87	6.90	Colombo			2.9	62°	-18°	-13°
2502	Chiang Mai	98.98	18.79							
2501	Bangkok	100.60	13.79							
2551	Penang	100.30	5.36	Penang			4.2	274°	174°	178°
2550	Kuala Lumpur	101.65	3.12	Klang	101.23	3.00	3.4	169°	67°	
2701	Saigon	106.70	10.78	Anam Hatien	104.45	10.37	13.0	45°	-62°	165°
4100	Bandung	107.63	-6.90	Jakarta	106.90	-6.10	13.5	120°	12°	
4210	Darwin	131.13	-12.85	Darwin			34.7	313°	182°	187°
4010	Baguio	120.58	16.41	San Fernando	120.30	16.60	20.1	276°	155°	154°
4011	Manila Obs.	121.07	14.64	Manila			28.0	278°	157°	156°
2555	Kota Kinabalu	116.07	5.95	Gaya	116.10	6.10	29.8	267°	151°	153°
4105	Banjar Baru	114.78	-3.33	Sungai Musang	114.50	-3.50	27.3	269°	154°	152°
4111	Manado	124.83	1.45	Gorontalo	123.10	0.50	10.4	227°	102°	109°
4120	Jayapura	140.67	-2.50	Hollandia			13.0	189°	48°	54°
4110	Ujung Pandang	119.63	-5.67	Macassar			17.0	278°	158°	157°
4115	Kupang	123.57	-10.20				10.4	328°	204°	163°
4160	Port Moresby	147.15	-9.41	Finsch Harb	147.80	-6.60	7.0	272°	125°	

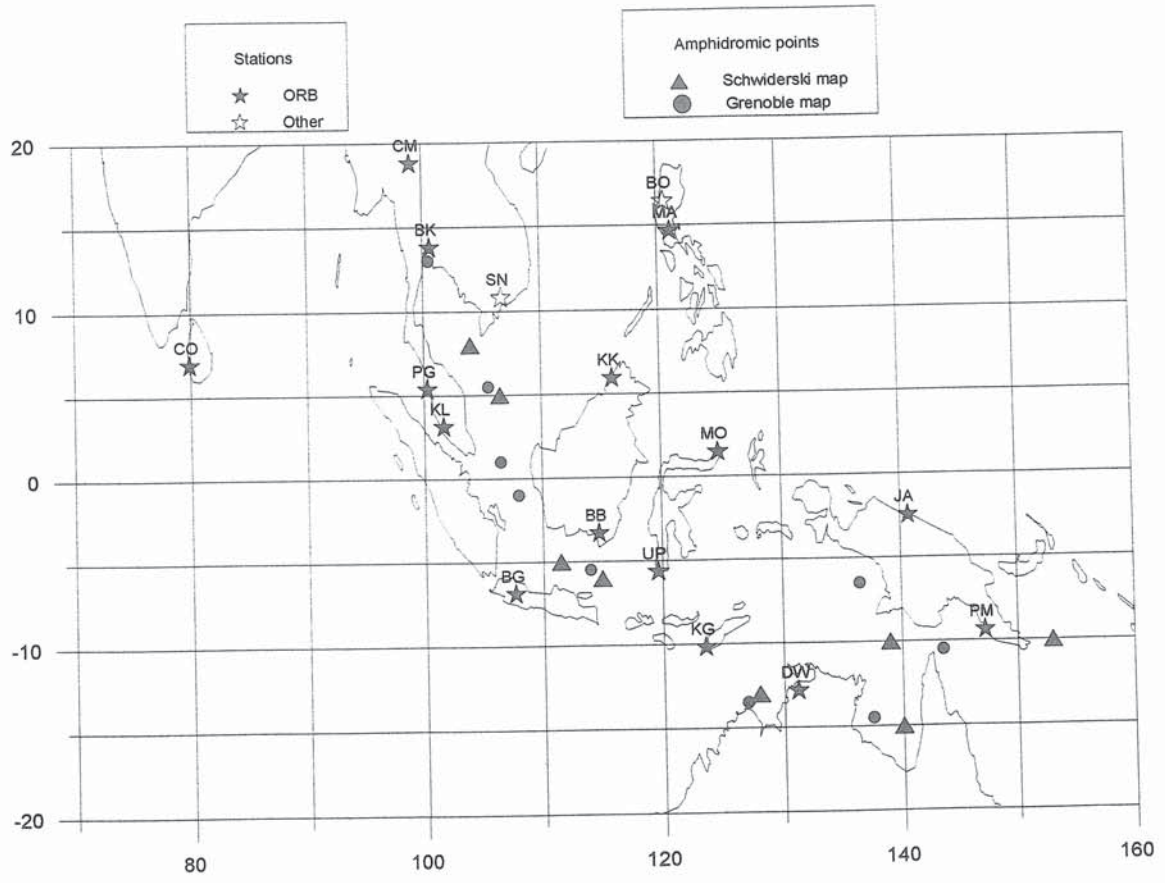

Figure 1 Geographical distribution of the tidal gravity stations and of the wave M_2 amphidromic points in the Schwiderski and in the Grenoble cotidal maps.

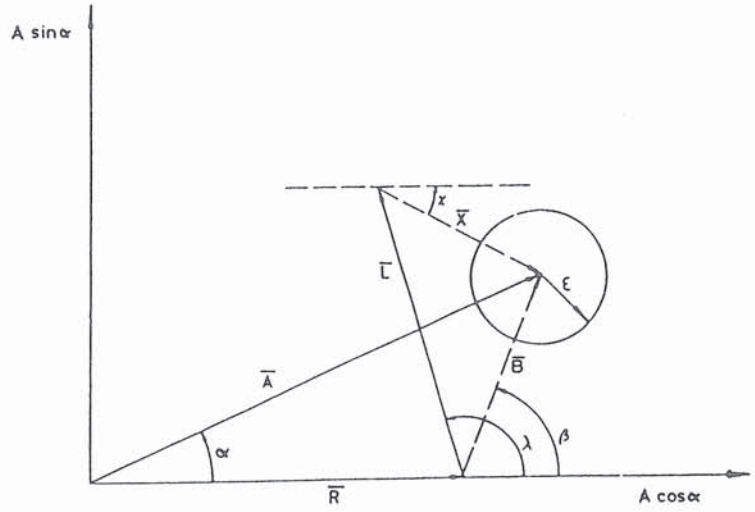

Figure 2 Definitions and notations: A (A, α), observed vector; R (R, 0), elastic oceanless earth model response (calculated); B (B, β) = A - R; L (L,) λ), oceanic attraction and loading vector (calculated); X (X, χ) = B - L = A - R - L final residue; ϵ, noise level approaching 0.3 μgal; X greater than ϵ ?

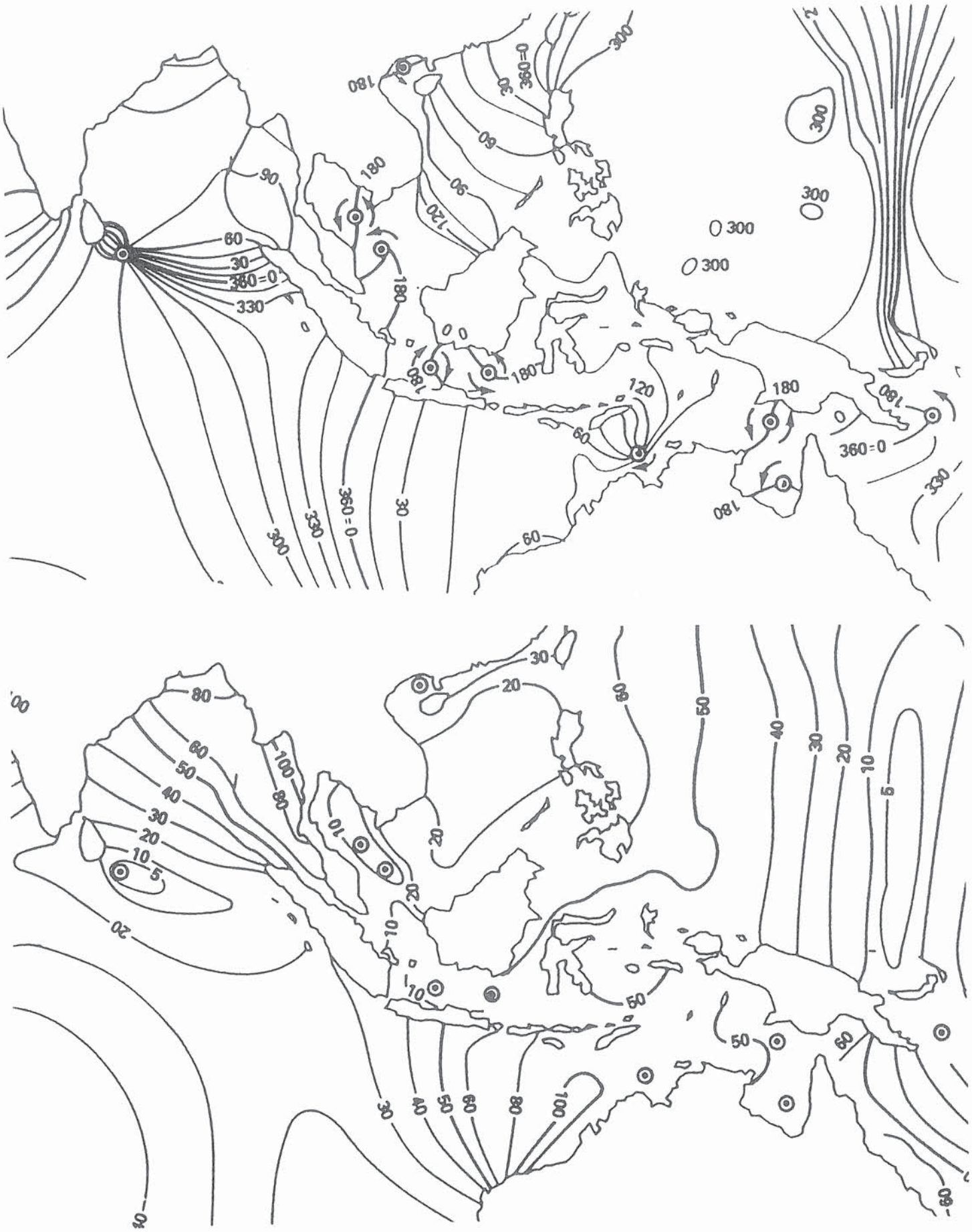

Figure 3 M_2 wave cotidal and corange maps according to Schwiderski (1979).